Research Article

Petroleum and Chemical Industry International

Determination of Shale Volume, Shale Types and Effective Porosity Based On Cross Plotting

Ghassem Al-Askari MK* and Roozmeh Ali

Petroleum University of Technology, Ahwaz, Iran

***Corresponding author**
Ghassem Al-Askari MK, Petroleum University of Technology, Ahwaz, Iran, E-mail: ghassemal@gmail.com

Submitted: 10 Sep 2018; **Accepted**: 17 Sep 2018; **Published**: 25 Oct 2018

Abstract

The evaluation of shaley formations has long been a difficult task. Presence of shale and shale types in some of the Iranian formations are one of the most important factors. Shale types have to be considered, because existence of shale reduces, porosity and permeability of the reservoir to some degree. Shale Distributed in formations in three basic types, Dispersed, Laminar and structural. Each of these shale types has different effect on porosity, permeability and saturation. Dispersed shale reduces porosity and permeability to a great degree, but, laminar shale and structural shale have little effect on petrophysical parameters. In this investigation, shale types, Shale volume and effective porosity of Kangan Formation have been determined from well log data and compared with crossplotting. In other words, a triangle Density-Neutron cross-plot is used to determine above parameters. The area of study lies in central oil fields of Iran, where one of the well is used (Tabnak Well C). Tabnak Well C selected to study Kangan Formation from Iranian oil field, in Pars onshore. This study illustrates that distribution of shale types in Kangan Formation is mainly dispersed shale with few of laminar shale, and percentage of effective porosity (φ_e) decreases with increasing depths for Kangan Formation.

Keywords: Crossplotting, Shale volume, Shale types, Effective porosity, Kangan Formation, Iran

Introduction

Shale is a sedimentary rock composed of almost, 50 % silts, 35 % clay minerals and 15 % fine and heavy classic particles. Considerable portion of shale consists of clay minerals such as illite, kaolinite, chlorite, montmorillonite, and etc. Clay minerals in the reservoir formation can change the petrophysical properties and reduces effective and total porosity and permeability of the reservoir [1]. Also, shale causes serious problems in formation evaluation and drilling operations [2].

Shale is distributed in reservoir formations in three basic types, structural, laminar, dispersed or combination of these three types [3]. Each type of shale is described as given in Ghorab, 2008 [4].

Structural shale exists in the form of fragments or crystals which are an integral part of the rock framework and, is considered as a portion of rock matrix. This type of shale has little effect on porosity or permeability [5].

Laminar shale exists as layer of clay minerals within clean formations (i.e. sandstone, carbonate, etc). The effect of this type of shale on porosity and permeability is severe and should be investigated.

Dispersed shale is composed of clay minerals, fragments or crystals which found on grain surface, occupying pore spaces between matrix and particles. Dispersed shale may include both detritus and digenetic clays. One or both of these forms may be present in dispersed shale. This type of shale reduces effective porosity and permeability to a great degree [6].

Shale also in general affects all well logging measurements to some degree [7]. Using well logging data, presence of shale in any formation can be recognized. Besides, shale type and shale volume can be determined either graphically (by cross plotting) or analytically [8].

Determination of Shale Volume

In this investigation, V_{sh} estimated from cross plotting and is validated with V_{sh} calculated from Gamma ray spectrum. Gamma ray spectrum is the best and most accurate method for determining shale volume, but not the shale types. The following equations are used to determine shale volume [9]:

$$IGR = \frac{GR_{log} - GR_{min}}{GR_{max} - GR_{min}} \quad (1)$$

- **IGR** is the Gamma ray index,
- $\mathbf{GR_{log}}$ is the gamma ray response in the zone of interest
- $\mathbf{GR_{min}}$ is the gamma ray response in cleanest formation
- $\mathbf{GR_{max}}$ is the gamma ray response in shale layer

Then, the shale volume (V_{sh}) can be calculated from the Gamma ray index, by the following formula:

$V_{sh} = 0.33[2^{(2\times IGR)}-1.0]$ for older rocks (2)
$V_{sh} = 0.083[2^{(3.7\times IGR)}-1.0]$ for Tertiary rocks (3)
$V_{sh} = IGR / [3 - 2IGR]$ (4)

Note that, the equation (4) is applied for this study and compared with cross plotting.

Hydrocarbon Correction

More accurate method to correct for hydrocarbon effect on density and neutron porosities is before points are plotted on cross plot [10]:

For the neutron porosity

$$\varphi Ncorr = \varphi N - \Delta\varphi N \quad (5)$$

Where

$$\Delta\varphi N = \varphi S_{hr} \frac{\rho_h - 0.7 + 0.4P}{1 - 0.4P} \quad \text{for oil} \quad (6)$$

$$\Delta\varphi N = \varphi S_{hr} \frac{2.2\rho_h - 1.0 + 0.4P}{1 - 0.4P} \quad \text{for gas} \quad (7)$$

In fresh mud (less than 50000PPM) the above equations can be reduced to:

$\Delta\varphi N = \varphi Shr\ (\rho h - 0.7)$ for oil (8)
$\Delta\varphi N = \varphi Shr\ (2.2\rho h - 1.0)$ for gas (9)

And,

- **P** is salinity of the mud in PPM
- **φN** is neutron porosity
- φ_{Ncorr} is corrected neutron porosity
- ρ_h is hydrocarbon density
- S_{hr} is residual oil saturation

For the density porosity

$$\varphi_{dcorr} = \varphi_d - \Delta\varphi_d \quad (10)$$

Where,

$$\Delta\varphi_d = 1.07\varphi S_{hr} \frac{(1.11(1-\rho_h) + 0.65P - 0.03)}{\rho_{ma} - 1.0 - 0.7P} \quad \text{for gas} \quad (11)$$

$$\Delta\varphi_d = 1.07\varphi S_{hr} \frac{1.11 - 0.65P - 1.24\rho_h}{\rho_{ma} - 1.0 - 0.7P} \quad \text{for oil} \quad (12)$$

In salinity less than 50000 PPM (fresh mud) P can be considered 0. And,

- φ_N is density porosity
- φ_{Ncorr} is corrected density porosity

An estimated of hydrocarbon density ρ_h can be obtained by the following equations:

$$\rho h = \frac{0.7\times\left(1+\frac{\varphi_N}{\varphi_d}\right)S_{hr} - \left(1-\frac{\varphi_N}{\varphi_d}\right)}{\left(1+0.72\frac{\varphi_N}{\varphi_d}\right)S_{hr}} \quad \text{for oil} \quad (13)$$

$$\rho h = \frac{\left(1+0.72\frac{\varphi_N}{\varphi_d}\right)S_{hr} - \left(1-\frac{\varphi_N}{\varphi_d}\right)}{\left(2.2+0.8\frac{\varphi_N}{\varphi_d}\right)S_{hr}} \quad \text{for gas} \quad (14)$$

Residual hydrocarbon saturation used, because the neutron and density tools investigate the flushed zone. The portion of hydrocarbon in the clean zone is given by Archie's equation [12]:

$$S_{xo} = \sqrt{\left(\frac{a}{\varphi^m} \times \frac{R_{mf}}{R_{xo}}\right)} = \sqrt{\frac{FR_{mf}}{R_{xo}}} \quad (15)$$

And

$$S_{hr} = 1 - S_{xo} \quad (16)$$

Where,

- φ is porosity of the formation
- m is cementation factor
- a is lithology constant
- R_{mf} is resistivity of mud filtrate
- R_{xo} is resistivity of flushed zone(micro resistivity tools response)

Porosity cross plot is an important analysis technique for determining petrophysical parameters. In this study a triangle neutron-density porosity cross plot (Fig.1) has been used to determine shale types, shale volume and effective porosity of any formation.

In this cross plot three distinct points (F, M, Sh) are shown (Fig. 1). Point **F** represents fluid or water point where φD= φN=100%. Point **M** represents matrix point. If density and neutron tools are calibrated in term of the existing matrix, then $\varphi_N = \varphi_D = 0$. Point **SH** represents shale point. The coordinate of point **SH** [φ_{NSh}, φ_{DSh}] must be determine for shaley portion of well and this coordinate vary from well to well and have to be estimated for each interval.

Line **M-F** represents border of clean formation or V_{sh}=0 line. This line is scaled in effective porosity as shown in Fig. 1. Points representing φ_N and φ_D values in clean formations will fall on above **M-F** line and their position on the line indicate effective porosity values. Line **M-Sh** represents $\varphi_e = 0$ line and value of each point on this line indicates shale volume of the formation that has no effective porosity. Points that represent shaley formation fall within triangle. Because porosity values do not exceed 50%, line **M-F** is plotted till 50% porosity to make full use of cross plot [2,13].

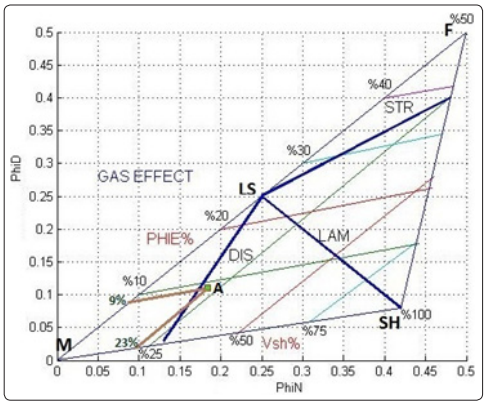

Figure 1: Neutron-Density porosity cross-plot

Following equations can be used to construct effective porosity, shale volume and shale type by using triangle cross plotting [10]:

$$\varphi_e N = \varphi N - (\varphi_{NSh} \cdot V_{sh}),\ \varphi_e D = \varphi D - (\varphi_{DSh} \cdot V_{Sh}) \quad (17)$$

The laminar shale points fall on LS-Sh or around of **LAM** line, dispersed shale points lie in the left of the line (around of **DIS** line)

and structural shale points lie in the right of the line (around of **STR** line) (Fig 1). For each point within triangle V_{Sh} is estimated on M-Sh line parallel to clean formation line, and also, φ_e is determined on clean formation line parallel to **M-Sh** line. For example point **A** in Fig.1 represents a shaley formation that has values of φ_e = 9% and VSh = 23%. Shale type for this point is dispersed shale.

If formation contains gas, Neutron and Density porosities have to be corrected before points are plotted.

Results and Discussion

There have been six depths interval of Tabnak Well-C selected to study kangan Formation. For choosing these intervals one has been tried that selected sections of the formation have different volume of shales. The results for each interval have been given below:

1-Depth interval "2590-2592m"

This interval of formation has considerable volume of shale and saturated with formation water (Fig.2). After plotting measured points of this interval on cross plot (Fig.3), is seen that aggregation of points is around laminar shale line. So, distribution mode of shale for this section of formation is laminar shale. V_{sh} and φ_e estimated from cross plot for each point of this interval are tabulated in Table 1.

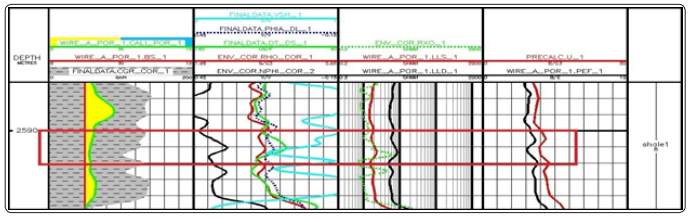

Figure 2: full set log data for depth interval 2590-2592m

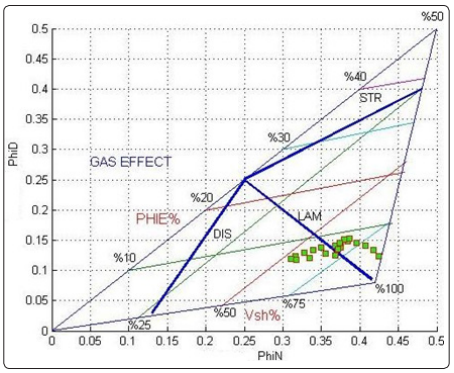

Figure 3: Neutron-Density porosity crossplot for depth interval 2590-2592m

Table 1: V_{sh} and φ_e estimated from crosplot for depth interval 2590-2592m

PHI-N	PHI-D	PHIE-CP %	VSH-CP
0.424	0.122	0.051	0.88
0.417	0.133	0.067	0.83
0.407	0.141	0.079	0.78
0.395	0.145	0.085	0.73
0.375	0.144	0.090	0.67
0.367	0.141	0.088	0.66
0.350	0.137	0.088	0.62
0.339	0.133	0.085	0.60
0.328	0.128	0.081	0.58
0.315	0.123	0.087	0.56
0.309	0.119	0.074	0.56
0.317	0.117	0.070	0.58
0.335	0.120	0.069	0.63
0.355	0.127	0.074	0.67
0.374	0.138	0.082	0.69
0.384	0.148	0.092	0.69
0.387	0.153	0.098	0.68
0.379	0.152	0.098	0.67
0.373	0.144	0.091	0.67
0.371	0.134	0.078	0.69
0.365	0.125	0.067	0.71

2-Depth interval "2650.3-2652"

This section has no shale and there is gas in formation (Fig.4). So, neutron and density porosities must be corrected for hydrocarbon effect. Fig.5 and Fig.6 shown position of points before and after correcting hydrocarbon effect for neutron and density porosities on cross plot and is seen that points fall on clean formation line after hydrocarbon correction. For this interval, φ_e estimated from cross plot correspond to 15.2 to 16.6 % (Table.2) and effective porosity measured with core analysis method is 17.1 to 18.2%. As can be seen, this result is very close together, therefore, this method can be applied to estimate effective porosity with acceptable accuracy. V_{sh} and φ_e determined from cross plot for each point of this interval are tabulated in Table 2.

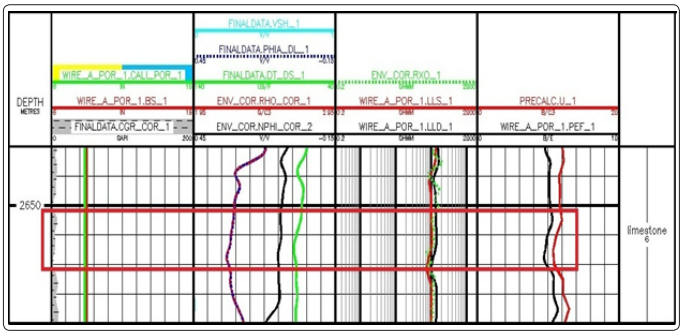

Figure 4: full set log data for depth interval 2650.3-2652m

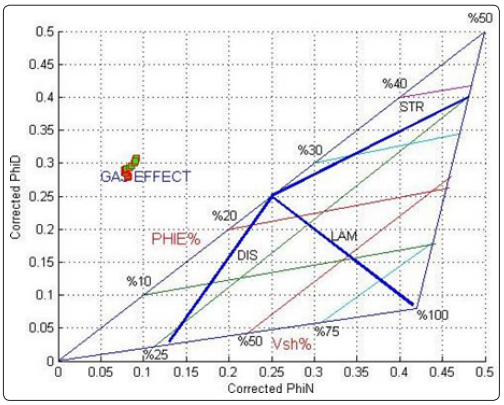

Figure 5: Neutron-Density porosity crossplot for depth interval 2650.3-2652m (before gas correction).

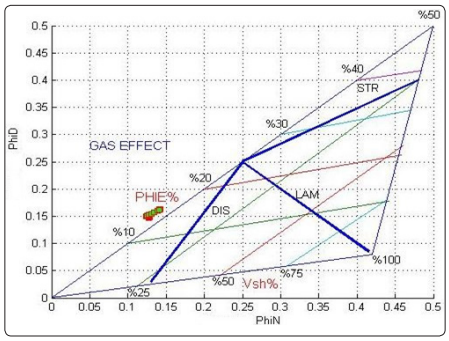

Figure 6: Neutron-Density porosity cross plot for depth interval 2650.3-2652m (after gas correction).

Table 2: v_{sh} and φ_e estimated from crosplot for depth interval 2650.3-2652m

PHIN-COR	PHID-COR	PHIE-CP	VSH-CP	VSH-GR
0.127	0.147	0.152	0	0
0.127	0.148	0.152	0	0
0.128	0.148	0.153	0	0
0.127	0.149	0.153	0	0
0.126	0.149	0.154	0	0
0.125	0.150	0.155	0	0
0.124	0.150	0. 156	0	0
0.124	0.150	0.156	0	0
0.125	0.151	0.157	0	0
0.127	0.152	0.158	0	0
0.130	0.153	0.159	0	0
0.134	0.156	0.161	0	0
0.138	0.159	0.164	0	0
0.141	0.162	0.167	0	0
0.142	0.163	0.168	0	0

3-Depth interval "2718.5-2719.5m":

This interval of formation has intermediate volume of shale and saturated with formation water (Fig.7). After plotting measured points of this interval on crossplot (Fig.8) is seen that points occupy the area between laminar and dispersed shale lines. So, distribution mode of shale for this section of formation is combination of laminar and dispersed shale types (mostly of laminar shale). V_{sh} and φ_e estimated from crossplot for each point of this interval are tabulated in Table 3.

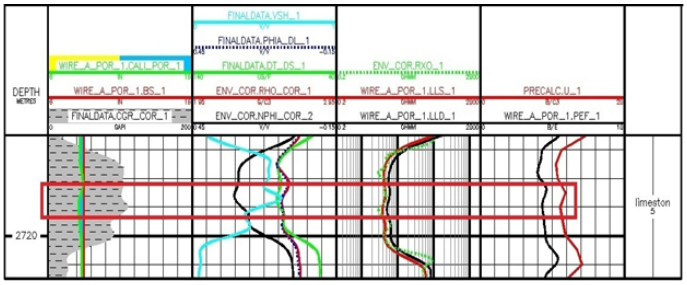

Figure 7: full set log data for depth interval 2718.5-2719.5m

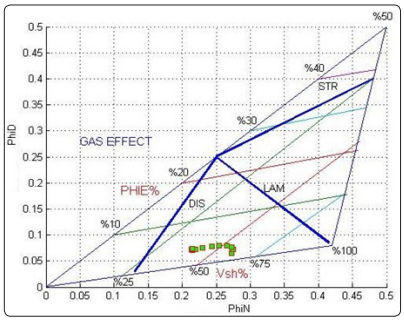

Figure 8: Neutron-Density porosity crossplot for depth interval 2718.5-2719.5m.

Table 3: V_{sh} and φ_e estimated from crosplot for depth interval 2718.5-2719.5m

PHI-N	PHI-D	PHIE	VSH-CP	VSH-GR
0.272	0.065	0.017	0.607	0.557
0.274	0.072	0.024	0.595	0.604
0.272	0.077	0.031	0.574	0.620
0.264	0.079	0.036	0.545	0.593
0.254	0.079	0.038	0.513	0.534
0.244	0.077	0.038	0.489	0.466
0.230	0.074	0.038	0.458	0.411
0.219	0.071	0.037	0.434	0.376
0.214	0.071	0.037	0.422	0.363
0.214	0.072	0.038	0.418	0.368
0.215	0.074	0.040	0.414	0.384

Comparing V_{sh} estimated from crossplot and V_{sh} calculated from Gamma ray method (using CGR data), these values are very close together for each point(Fig.9), therefore, crossplot method can be used to determine shale volume, shale type and effective porosity with acceptable accuracy. This comparison has been done for other intervals.

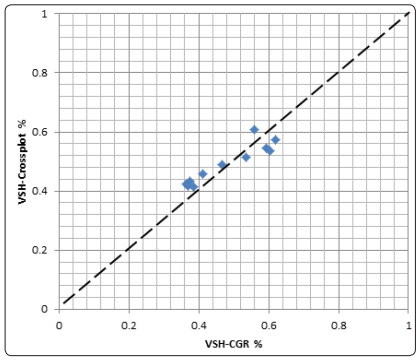

Figure 9: V_{sh} estimated from crossplot method VS. V_{sh} from Gamma ray spectrum for depth interval 2718.5-2719.5m

4-Depth interval "2730.5-2731.5m":

This section of formation has intermediate volume of shale and saturated with formation water (Fig.10). After plotting measured points of this interval on crossplot (Fig.11) is seen that aggregation of points is around dispersed shale line. So, distribution mode of shale for this section of formation is dispersed. V_{sh} and φ_e estimated

from crossplot for each point of this interval are tabulated in Table 4. Degree of match between CGR and Crossplotting is shown in Fig.12. As one can see in Fig.12 the degree of match between CGR and Crossplotting is reduced, compare to Fig.9, because the dispersed shale (25%) in this interval causing neutron log dispersion.

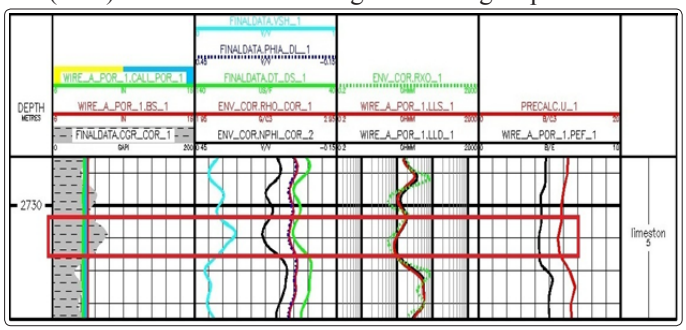

Figure 10: full set log data for depth interval 2730.5-2731.5m.

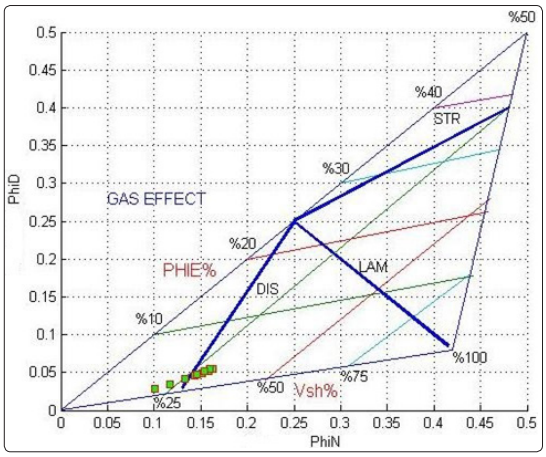

Figure 11: Neutron-density porosity cross plot for depth interval 2730.5-2731.5m.

Table 4: V_{sh} and φ_e estimated from crosplot for depth interval 2730.5-2731.5m

NPHI	PHID	PHIE-CP	VSH-CP	VSH-GR
0.142	0.045	0.022	0.286	0.207
0.151	0.049	0.024	0.302	0.239
0.158	0.052	0.027	0.312	0.270
0.162	0.054	0.028	0.319	0.289
0.163	0.055	0.029	0.318	0.289
0.159	0.054	0.029	0.310	0.272
0.154	0.051	0.027	0.301	0.247
0.145	0.047	0.024	0.288	0.224
0.132	0.041	0.019	0.270	0.205
0.117	0.034	0.014	0.243	0.190
0.100	0.027	0.011	0.214	0.171

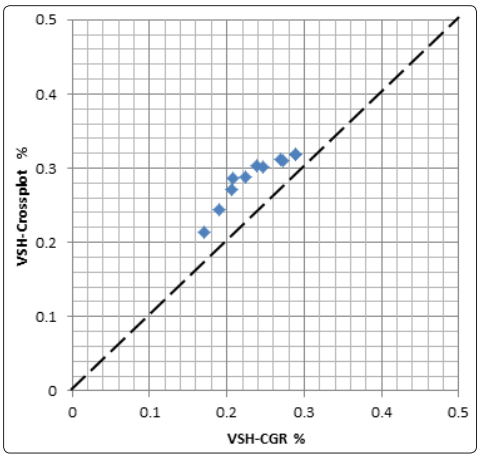

Figure 12: V_{sh} estimated from cross plot method VS. V_{sh} from Corrected Gamma Ray spectrum (CGR) for depth interval 2730.5-2731.5m

5-Depth interval "2743-2744m"

This interval of formation has low volume of shale and saturated with formation water (Fig.13). After plotting measured points of this interval on cross plot (Fig.14) is seen that aggregation of points is around dispersed shale line. So, distribution mode of shale for this section of formation is dispersed. V_{sh} and φ_e estimated from cross plot for each point of this interval are tabulated in Table 5. Correlation between CGR and Cross plotting is shown in Fig.15. As one can see in Fig.15 the degree of match between CGR and Cross plotting is good, compare to Fig.12, because the dispersed shale (12%) in this interval is not causing neutron log dispersion.

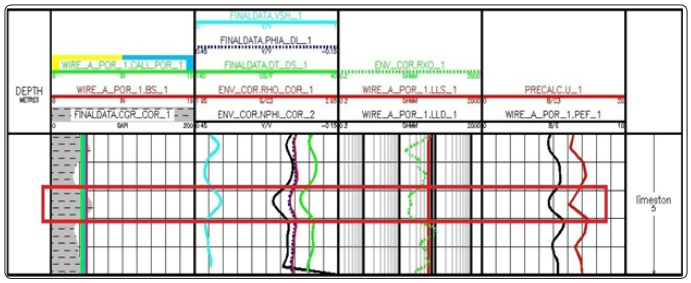

Figure 13: full set log data for depth interval 2743-2744m

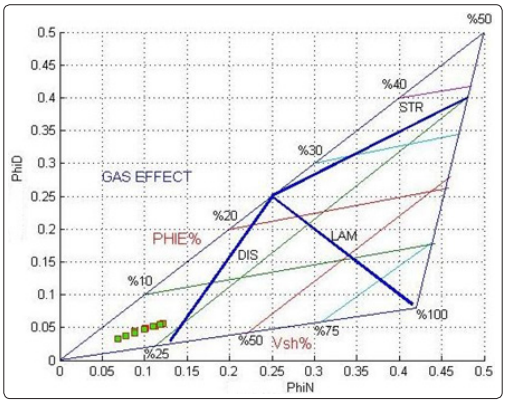

Figure 14: Neutron-density porosity crossplot for depth interval 2743.-2744m

Table 5: V_{sh} and φ_e estimated from crosplot for depth interval 2743-2744m

NPHI-COR	PHID-COR	PHIE-CP	VSH-CP	VSH-GR
0.087	0.043	0.033	0.128	0.136
0.100	0.048	0.036	0.152	0.155
0.112	0.052	0.038	0.174	0.171
0.119	0.055	0.040	0.189	0.181
0.121	0.056	0.041	0.193	0.184
0.118	0.055	0.040	0.186	0.178
0.110	0.052	0.038	0.171	0.165
0.099	0.047	0.035	0.152	0.146
0.088	0.041	0.031	0.136	0.125
0.077	0.036	0.026	0.121	0.106
0.068	0.032	0.024	0.105	0.090

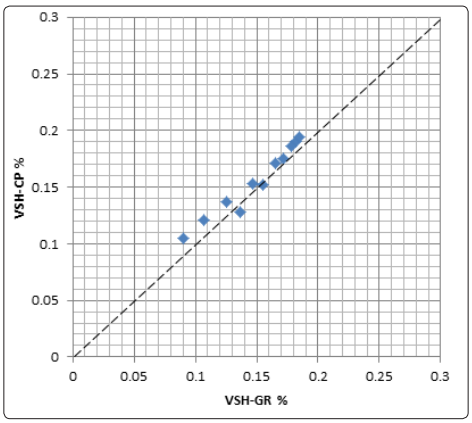

Figure 15: V_{sh} estimated from crossplot method VS. V_{sh} from Gamma ray Spectrum for depth interval 2743-2744m

Conclusion

There are five depth intervals of Well C in kangan Formation of Tabnak oil field, central Iranian oil field, presented here using of cross plotting methods. Types of shale for each interval, shale volume and effective porosity for each point of intervals have been estimated. A triangle neutron-density porosity cross plot has been applied for this purpose.

Shale volume, V_{sh}, estimated from crossplot method has been validated with V_{sh} calculated from Gamma ray method by using Strieber's (1970) equation [11]. Also, φ_e estimated from cross plot method has been compared with φ_e measured from core analysis or log analysis.

This study illustrates that distribution mode of shale in Tabnak well C of kangan Formation is mainly dispersed with few of laminar. Based on effective porosity estimated from cross plot, reservoir quality decreases with increasing in depth along the kangan Formation.

Besides, shale volume cross plot method showed that in case of high volume of dispersed shale (more than 12%), there is high neutron log dispersion effect on neutron porosity. Also seen that these compared values are very close together, therefore, cross plotting methods can be used to determine shale volume, shale types, effective porosity and neutron log dispersion effect with acceptable accuracy.

Cross plotting method can be used for any formation, but properties of shaley layers (i.e. φNSh , φDSh) in study area should be determined and recalibrated after few wells have been drilled.

Cross plotting methods are quick and commodious methods in comparison with other methods such as log analysis or log interpretation for determining petrophysical parameters.

The results of these methods can be used to estimate productivity and capacity of the reservoir.

References

1. Tiab D, Donaldson EC (2004) Petrophysics: Theory and Practice of Measuring Reservoir Rock and Fluid Transport Properties (second edition Ed.). Gulf Professional Publishing.
2. Bassiouni Z (1994) Theory, measurement, and interpretation of well logs. richardson, texas: Henry L. Doherty Memorial Fund of AIME, Society of Petroleum Engineers.
3. Worthington PF (1985) The Evolution of Shaly-sand Concepts in Reservoir Evaluation. The Log Analyst 26: 23-40.
4. Ghorab M, Ramadan MA, Nouh A (2008) The Relation Between the Shale Origin (Source or non Source) and its Type for Abu Roash Formation at Wadi El- Natrun Area, South of Western Desert, Egypt. Australian Journal of Basic and Applied Sciences 2: 360-371.
5. Ruhovets N, Fertl WH (1982) Volumes, Types, and Distribution of Clay Minerals in Reservoir Rocks Based on Well Logs. SPE Unconventional Gas Recovery Symposium, Pittsburgh, Pennsylvania 64-79.
6. Ghassem-Alaskari MK (2012) Analysis of Shaley reservoir zones and their effects on logging tools for Interpretation of Reservoir Parameters in Coastal Fars fields of Iran. ICOFC, Iran.
7. Serra O (1984) fundamentals of well-log interpretation (first edition Ed.) New York: ELSEVIER SCIENCE PUBLISHING COMPANY INC.
8. Ghassem Alaskari MK, oozmeh A (2017) Determination of Shale Types using Well Logs, International Journal of Petrochemical Science & Engineering 2: 5.
9. Dresser Atlas (1982) well logging and interpretation techniques. houston, texas: Dresser ind, inc.
10. Brock j (1986) Applied open- hole log analysis (Vol. 2) houston, texas: gulf publishing company.
11. Stieber S (1970) Pulsed Neutron Capture Log Evaluation - Louisiana Gulf Coast. SPE paper 2961, Fall Meeting of the Society of Petroleum Engineers of AIME, 4-7 October. Houston, Texas.
12. Archie G (1942) The Electrical Resistivity Log as an Aid in Determining Some Reservoir Characteristics. Transactions of the AIME 146: 54-62.
13. Bigelow E l (1992) Introduction to Wireline Log Analysis. Houston, Texas: Western Atlas International, Inc.